Limiting behavior of the probability distribution in Einstein's bed-load formula and its improvement

Wu, Haoliang; Cheng, Nian-Sheng; Chiew, Yee-Meng

2021

Wu, H., Cheng, N. & Chiew, Y. (2021). Limiting behavior of the probability distribution in Einstein's bed-load formula and its improvement. Water Resources Research, 57(10), e2020WR028900-. https://dx.doi.org/10.1029/2020WR028900

https://hdl.handle.net/10356/153676

https://doi.org/10.1029/2020WR028900

AGU ADVANCING EARTH AND SPACE SCIENCE

Water Resources Research®

RESEARCH ARTICLE
10.1029/2020WR028900

Limiting Behavior of the Probability Distribution in Einstein's Bed-Load Formula and its Improvement

Haoliang Wu[1], Nian-Sheng Cheng[2], and Yee-Meng Chiew[1]

[1]School of Civil and Environmental Engineering, Nanyang Technological University, Nanyang, Singapore, [2]Ocean College, Zhoushan Campus, Zhejiang University, Zhoushan, China

Key Points:

- The weakness of Einstein's formula in predicting very low and high transport rates is inherent in the presumed probability distribution
- The range of validity of the Einstein-type bed-load formula's is improved by using Gamma distribution
- The limiting forms of the improved formula agree well with the extreme trends of data in the very low and high transport regimes

Correspondence to:
N.-S. Cheng,
nscheng@zju.edu.cn

Citation:
Wu, H., Cheng, N.-S., & Chiew, Y.-M. (2021). Limiting behavior of the probability distribution in Einstein's bed-load formula and its improvement. *Water Resources Research*, *57*, e2020WR028900. https://doi.org/10.1029/2020WR028900

Received 22 SEP 2020
Accepted 19 AUG 2021

Abstract The bed-load transport rates predicted using Einstein's formula in the low and high transport regimes deviate from the experimental data. The deviation, which becomes significant when the transport rate is extremely low or high, may be solely attributed to the folded Gaussian distribution assumed by Einstein. The trends of an Einstein-type formula at the limits can be separately determined by considering the limiting behavior of the embedded probability distribution, which facilitates the derivation of a formula that best fits the bed-load data. By applying a Gamma distribution with the shape parameter equal to 3/2, a modified Einstein's formula is successfully applied to the low and high transport regimes.

1. Introduction

Einstein (1942) proposed two dimensionless parameters to evaluate bed-load transport rates, namely the intensity of bed-load transport Φ and flow intensity Ψ, which were defined, respectively, as

$$\Phi = \frac{q_B}{\sqrt{\Delta g D^3}} \tag{1}$$

$$\Psi = \frac{\Delta g D}{U_*^2} \tag{2}$$

where q_B is the volumetric bed-load transport rate per unit channel width, Δ is the submerged specific gravity, g is the gravitational acceleration, D is the average grain size which can be valued as D_{50}, median of the particle size distribution, and U_* is the shear velocity. It is noted that Ψ is the reciprocal of the Shields parameter Θ.

To devise a probabilistic model of bed-load transport, Einstein (1950) introduced the exchange probability p, which was defined as the probability of particle entrainment. It was further assumed that

$$p = \mathrm{P}\left(F_L > W'\right) \tag{3}$$

in which F_L is the fluctuating hydrodynamic lift force on a bed particle, W' is the submerged grain weight, and P denotes the probability function. Einstein's derivation of the stochastic bed-load model comprises two major steps: (1) the bed-load transport rate q_B is calculated from the entrainment rate of bed-load particles, that is, E, multiplied by their average consecutive travel distance, that is, L, as

$$q_B = EL \tag{4}$$

The volume of particles entrained per unit time from a unit area is calculated by

$$E = \frac{A_2 D^3}{A_1 D^2}\frac{p}{t_*} = \frac{(A_2/A_1)Dp}{A_3 D/\sqrt{\Delta g D}} = A' p\sqrt{\Delta g D} \tag{5}$$

in which A_1 and A_2 are the constants for the area and volume of a particle, $t_* = A_3 D/\sqrt{\Delta g D}$ is the sediment exchange time that scales with the time for a settling sediment to fall a distance of D, in which A_3 is the scale constant of t_*, and $A' = A_2/(A_1 A_3)$. The average particle travel distance is calculated by

$$L = \frac{L_0}{1-p} = \frac{A_L D}{1-p} \tag{6}$$

in which L_0 is the average distance of a single saltation step and A_L is the scale constant of L_0. Both E and L are characterized by p, therefore $\Phi(p)$ is obtained as

$$\Phi = \frac{1}{A_*}\frac{p}{1-p} \tag{7}$$

or

$$p = \frac{A_*\Phi}{1 + A_*\Phi} \tag{8}$$

where $A_* = (A'A_L)^{-1}$ is the compound constant in $\Phi(p)$.

Then, (2) the probability distribution of $F_L > W'$ is determined by the flow intensity Ψ, which can be regarded as the scale of the ratio of W' to F_L:

$$\Psi = \frac{\Delta g D^3}{U_*^2 D^2} \sim \frac{W'}{F_L} \tag{9}$$

To achieve this goal, F_L was expressed by Einstein (1950) as

$$F_L = \overline{F_L}\left(1 + \eta_0\eta_*\right) \tag{10}$$

where $\overline{F_L}$ is the average hydrodynamic lift force, η_0 is the relative standard deviation of F_L, and η_* is a normalized dimensionless random variable characterizing F_L. Thus, p was determined as

$$p = \mathrm{P}(\mid 1 + \eta_0\eta_* \mid > B'\Psi) \tag{11}$$

in which B' is a constant. In addition, Einstein (1950) defined $B_* = B'/\eta_0$ for the simplicity of the deterministic expression of $p(\Psi)$.

With this, Einstein (1950) derived the functional forms of $\Phi(p)$ and $p(\Psi)$. By assuming that η_* follows the standard Gaussian distribution and $\eta_0 = 0.5$, Einstein (1950) derived the bed-load formula $\Phi(\Psi)$ from the combination of Equations 7 and 11 as follows:

$$\Phi = \frac{1}{A_*}\left[\left(\frac{1}{\sqrt{\pi}}\int_{-B_*\Psi-1/\eta_0}^{B_*\Psi-1/\eta_0}\exp(-t^2)\mathrm{d}t\right)^{-1} - 1\right] \tag{12}$$

where the parameters were calibrated as $A_* = 43.50$ and $B_* = 0.143$.

However, Einstein's formula was actually not determined by using a probabilistic approach, since no probability distribution of any quantity was calculated (Ancey, 2020). In particular, the parameters in Einstein's formula were calibrated by fitting the transport rate data, in spite of the fact that Einstein (1950) associated them with the stochastic microscopic sediment motion. The statistical arguments in Einstein's model were likely to be used only to introduce the probability distribution function.

The formula from Einstein (1950) accurately predicted the bed-load transport rates of the experimental data cited in Einstein's study, of which Ψ lays within $1.5 < \Psi < 30$ and Φ lays within $10^{-4} < \Phi < 10$ (Einstein, 1950; Gilbert & Murphy, 1914; Meyer-Peter & Müller, 1948). However, subsequent researchers showed that Einstein's formula is patently inconsistent with the measurements of very low and high transport rates (Paintal, 1971; Wilson, 1966) that exceed the measurable range in Einstein's era. Moreover, Yalin (1972) calculated the limiting forms of Einstein's formula when the bed-load transport rate approaches zero and infinity, and found that the deviation between Einstein's formula and the experimental data increases when the transport rate approaches the extreme levels, viz., $\Phi \to 0$ and $\Phi \to \infty$. Yalin (1972) also showed that the trends of Einstein's formula at the limits do not depend on values of the parameters, which implies that the functional form of Einstein's formula needs to be modified.

As summarized in Table 1, many published studies have improved Einstein's formula by modifying Einstein's theoretical assumptions (Armanini et al., 2009, 2015; Chen et al., 1986; Yalin, 1972; Wang, 1985; Wang et al., 2008). On the one hand, most of the studies revised $\Phi(p)$ by improving the accuracy in evaluating E and L. While Einstein (1950) assumed that L_0 and t_* are not related to the flow intensity, Yalin (1972) stated that L_0 and t_* should be, respectively, proportional to Ψ^{-1} and $\sqrt{\Psi}$. Later studies (Armanini et al., 2009; Wang, 1985; Wang et al., 2008) also modified E and L, fully or partially, by following the suggestion of Yalin (1972). Furthermore, Yalin (1972) and Armanini et al. (2015) did not calculate E and L separately, but investigated the sediment transported through a cross section. Yalin (1972) assumed that the amount of sediments that can move the distance nL_0 in Nt_*, in which N is an integer that is, large enough, follows a Poisson

Table 1
Comparison Between the Functional Forms of Einstein's Bed-Load Formula and its Modifications[a,b,c]

	$\frac{E}{\sqrt{\Delta g D}}$	L/D	$p(\Psi)$	$\Phi(p)$
Einstein (1950)	$A'p$	$\frac{A_L}{1-p}$	$1-\frac{1}{\sqrt{\pi}}\int_{-B_*\Psi-1/\eta_0}^{B_*\Psi-1/\eta_0} e^{-t^2}\mathrm{d}t$	$\frac{1}{A_*}\frac{p}{1-p}$
Yalin (1972)	$\frac{EL}{\sqrt{\Delta g D^3}}=\frac{A_L\Psi^{-1}}{NA'^{-1}\Psi^{1/2}}\sum_{n=1}^{\infty}n\frac{(Np)^n}{n!}e^{-Np}$		$1-\frac{1}{\sqrt{\pi}}\int_{-\infty}^{B_*\Psi-1/\eta_0} e^{-t^2}\mathrm{d}t$	$\frac{p}{A_*\Psi^{3/2}}$
Wang et al. (2008)	$A'\Psi^{-1/2}p$	$\frac{A_L\Psi^{-1}}{1-p}$	$1-\frac{1}{\sqrt{\pi}}\int_{-\infty}^{B_*\Psi-1/\eta_0} e^{-t^2}\mathrm{d}t$	$\frac{1}{A_*\Psi^{3/2}}\frac{p}{1-p}$
Wang (1985)	$A'\Psi^{-1/2}p$	$\frac{A_L}{1-p}$	$1-\frac{1}{\sqrt{\pi}}\int_{-\sqrt{\frac{(1+\eta_{u'}^2)}{\eta_{u'}^2}}B_*\Psi-\frac{1}{\eta_{u'}}}^{\sqrt{\frac{(1+\eta_{u'}^2)}{\eta_{u'}^2}}B_*\Psi-\frac{1}{\eta_{u'}}} e^{-t^2}\mathrm{d}t$	$\frac{1}{A_*\Psi^{1/2}}\frac{p}{1-p}$
Armanini et al. (2009)	$A'\Psi^{-1/2}p$	$\frac{A_L}{1-p}$	$1-\frac{1}{\sqrt{\pi}}\int_{-B_*\Psi-1/\eta_0}^{B_*\Psi-1/\eta_0} e^{-t^2}\mathrm{d}t$	$\frac{1}{A_*\Psi^{1/2}}\frac{p}{1-p}$
Armanini et al. (2015)	$\frac{2A_u}{\Psi^{a+0.5}}p$	$\frac{K_1}{1+K_2\Psi}$	$1-\frac{1}{\sqrt{\pi}}\int_{-\infty}^{B_*\Psi-1/\eta_0} te^{-t}\mathrm{d}t$	$\frac{2A_uK_1p}{\Psi^{a+0.5}(1+K_2\Psi)}$

[a]N is a large enough integer in Yalin (1972). [b]$\eta_{u'}$ is the standard deviation of near-bed velocity in Wang (1985). [c]A_u, a, K_1, K_2 are parameters assumed by Armanini et al. (2015).

distribution whose intensity is Np. Armanini et al. (2015), however, assumed that the distribution of the sediment travel distances is a Gamma distribution and unrelated to p, and L/D is nonlinearly related to Ψ^{-1}. In summary, the functional forms of EL (i.e., $\Phi(p)$) evaluated by Yalin (1972) and Armanini et al. (2015) are shown in Table 1.

Researchers also modified the probability distribution that determines $p(\Psi)$ based on the assumed underlying physics of sediment entrainment. As shown in Table 1, Yalin (1972) and Wang et al. (2008) continued to assume that F_L has a Gaussian distribution, similar to Einstein (1950), but avoided using the absolute value of F_L to determine the sediment entrainment. Wang (1985), however, asserted that the fluctuating near-bed flow velocity u', rather than F_L, follows a Gaussian distribution. Thus, η_0 was replaced by the relative deviation of the flow velocity $\eta_{u'}$ and F_L was assumed to follow a Chi-square distribution. Armanini et al. (2015) used a Gamma distribution to describe p and claimed that the Gamma distribution stems from the statistics of sediment motion (Ancey et al., 2006) instead of the distribution of F_L. Armanini et al. (2015) did not applied the criteria of sediment entrainment used by previous studies, but the mechanism of sediment entrainment embedded in the proposed Gamma distribution was not clarified and is worth further investigation.

Nevertheless, some of the assumed underlying physics in the modified formulae may be found inaccurate, especially for the probability distributions used to determine p because the mechanisms of sediment entrainment have been updated in recent studies. For example, Schmeeckle et al. (2007) found that the hydrodynamic lift force on a bed particle is not linearly related to the square of velocities of its above flow. Thus, the Chi-square distribution may not accurately represent the fluctuation of F_L (Wang, 1985). Moreover, Celik et al. (2010) ascertained that the impulse of peak hydrodynamic force on a bed particle is a better criterion to determine sediment entrainment than the instantaneous hydrodynamic force. Thus, even if the probability distribution of F_L is accurate, it may not be used to directly evaluate p.

It is noticed that, despite the different physics implied in the different forms of $\Phi(p)$ and $p(\Psi)$, most of the foregoing bed-load formulae can accurately predict a wide range of bed-load transport rates (Armanini et al., 2015; Yalin, 1972; Wang, 1985). As commented by Ancey (2020), the calibration of the parameters in Einstein's formula by data fitting makes their physical meanings ambiguous. Therefore, it is not unreasonable to deduce that the assumed probability distributions (including the parameters) not only stem from the physics of sediment entrainment, but also involve considerations of data fitting. The limitation of this type

of formula is that they are difficult to be extended for predicting transport rates that exceed the range of data fitting (e.g., the fit attempted by Einstein (1950) for the limited data set available at his time cannot be repeated to the nowaday extended-range data set). Nonetheless, the determination of p through fitting the transport rate data is still inevitable until the sediment detachment frequency can be well measured under different flow conditions in the future (similar to Valyrakis et al. (2011)).

Since data fitting is almost inevitable at the current stage of sediment transport prediction, the type of probability distribution used in an Einstein-type formula, like the parameters, may also be determined empirically. Previous studies often presupposed the type of probability distribution, thus restricting the flexibility of their formula when fitting the data. For example, although Armanini et al. (2015) used a Gamma distribution which was often used in fitting the distributions based on undetermined physics (Ancey et al., 2006; Nicholas, 2000) because of its flexible form, they presupposed the parameters of the Gamma distribution before calibrating other parameters in their formulae. Previous researchers usually did not present an in-depth discussion in their publications on how the probability distribution was determined based on a data-driven consideration (e.g., Armanini et al., 2015; Einstein, 1950). It is reasonable to assume that most researchers implicitly analyzed the influence of their presumed probability distributions on data fitting (e.g., Yalin (1972) compared the limiting forms of his modified formula to the trends of data) but seldom clarified the analyses in their articles. Thus, it is worthwhile to analyze the general influence of an undetermined probability distribution on the data fitting of an Einstein-type formula. From this, a flexible framework can be obtained to determine the appropriate type of probability distribution to be used in fitting an Einstein-type formula to a wide range of bed-load data.

The present study, first, calculated the trends of Einstein's formula at the limits (similar to the analysis done by Yalin (1972)). This study further shows that they are determined by the type of probability distribution assumed by Einstein (1950). Then, to modify Einstein's probability distribution, a novel framework is proposed to derive the limiting behavior of the probability distribution that best fits the experimental data. Specifically, the gradients of the tails of a best fit probability distribution are approximated by fitting gradients of the $\Phi - \Psi$ data at the limits (which had been evaluated by Einstein (1942); Wilson (1966); Paintal (1971), and Cheng (2002)). It is found that a Gamma distribution can optimally match the tails of the best fit distribution. As a result, Einstein's formula is modified to be valid in $10^{-9} < \Phi < 300$, via fitting a Gamma distribution in $p(\Psi)$ to very low and high transport data and then adjusting the remaining parameter A_* in $\Phi(p)$. Moreover, the present modified formula is compared with the formula proposed by Armanini et al. (2015) and the possible physical meaning of the present Gamma distribution is discussed.

2. Limiting Behavior of Einstein's Probability Distribution

2.1. Reevaluation of Einstein's Probability Distribution

In accordance with Equation 11, Einstein (1950) defined the probability distribution based on η_*, which is a dimensionless parameter obtained by normalizing F_L. The aim of the present study, however, is to investigate the probability distribution through fitting the experimental data, without exploring the complex microscopic mechanism associated with the criterion of sediment pickup, for example, $F_L > W'$. Thus, the probability distribution implied in Equation 11 should be redefined based on a new dimensionless random variable, which can be compared with experimental data explicitly.

From the term $\left|1 + \eta_0\eta_*\right| > B'\Psi$ (Equation 11), it is found that only Ψ can be obtained from experimental data, and the other parameters depend on Einstein's assumptions. Thus, $\left|1 + \eta_0\eta_*\right| > B'\Psi$ is rearranged as $\left|\eta_* + 1/\eta_0\right|/B_* > \Psi$ to leave only Ψ on the right side. On the other hand, it is noted that $\left|\eta_* + 1/\eta_0\right|/B_*$ is dimensionless. If it is generalized as an undetermined parameter denoted by Ψ_*, $p(\Psi)$ can be written as

$$p = \mathrm{P}\left(\left|\eta_* + 1/\eta_0\right|/B_* > \Psi\right) = \mathrm{P}(\Psi_* > \Psi) = 1 - F_{\Psi_*}(\Psi) \tag{13}$$

where Ψ_* is regarded as a random variable upon which the probability distribution is defined. In this case, the microscopic criterion $F_L > W'$ is replaced by a macroscopic criterion to determine p, that is, $\Psi_* > \Psi$, so

that the probability distribution is associated with the relation $p - \Psi$, which can be obtained from experimental data. According to Equation 13, $p(\Psi)$ can be regarded as the complementary cumulative distribution function (1-CDF) of Ψ_*. In other words, $1 - p(\Psi)$ is treated as an undetermined distribution function.

Mathematically, every cumulative distribution function must be a nondecreasing and right-continuous function, and a distribution function can uniquely define a probability distribution. In other words, if a nondecreasing functional relation $1 - p(\Psi)$ is deduced from experimental data, the appropriate probability distribution of a bed-load formula can be uniquely determined. Based on the present consideration, this study investigates whether the Einstein-assumed distribution is a good approximation of the probability distribution that optimally fits experimental data, namely the best fit distribution, if no, how one can improve it.

Noting that Ψ_* is obtained by generalizing the expression in the Einstein-assumed $p(\Psi)$ (Equation 13), one may argue that Einstein (1950) had prespecified the probability distribution of Ψ_*. The assumed probability distribution is hence inferred by the corresponding expression of Ψ_*,

$$\Psi_* = \left| \frac{\eta_*}{B_*} + \frac{1}{B_* \eta_0} \right| \tag{14}$$

Einstein (1950) assumed that η_* follows the standard Gaussian distribution. According to Equation 14, it can be logically inferred that Ψ_* follows a folded Gaussian distribution, viz., being the module of a random variable with a Gaussian distribution, in which the mean and standard deviation are, respectively, $1/B_*\eta_0$ and $1/B_*$. Then, Einstein's assumptions of the probability distribution are combined and denoted as

$$\Psi_* = \left| X \right| \tag{15}$$

in which

$$X \sim \mathcal{N}\left(\mu = \frac{1}{B_* \eta_0}, \sigma = \frac{1}{B_*} \right) \tag{16}$$

where $\mathcal{N}(\mu, \sigma)$ represents a Gaussian distribution, μ is the mean, and σ is the standard deviation.

Without presupposing the specific values of μ and σ, the following sections, Sections 2.2 and 2.3, solely investigate the influence of the type of probability distribution presumed by Einstein (1950), viz., the folded Gaussian distribution $\left| X \right|$, on the discrepancies between Einstein's bed-load formula and some classic experimental datasets. The comparison between the original formula and the experimental data is presented in two ways: (1) analysing the plot of $\log \Phi - \log \Psi$, through which the inconsistency with the experimental data is patently shown; and (2) comparing the probability density function (PDF) plots of the folded Gaussian distribution and a best fit probability distribution deduced from the experimental data, which indicates how the probability distribution in an Einstein-type formula should be revised to improve the goodness-of-fit. Besides, it needs to be noticed that because the present analyses mainly focus on the trends of data and the functional form of the probability distribution, $\log \Phi - \log \Psi$, which is used in plotting, and $\ln \Phi - \ln \Psi$, which is used in calculations, are treated as identical in the following paragraphs without further explanation.

2.2. Comparison of the Relation $\ln \Phi - \ln \Psi$

Figure 1, which is presented on a double-log graph of $\Phi(\Psi)$, viz., $\log \Phi - \log \Psi$, shows the comparison between Einstein's bed-load Formula (Equation 12) and the compiled experimental data obtained from laboratory measurements (Gilbert & Murphy, 1914; Meyer-Peter & Müller, 1948; Paintal, 1971; Taylor & Vanoni, 1972; Wilson, 1966). In addition, some empirical bed-load formulae are also superimposed, including the exponential formula fitted with low bed-load transport rates proposed by Einstein (1942), the amended Meyer-Peter and Müller (1948) (MPM) formula fitted with high shear conditions (Wilson, 1966), and two power functions that, respectively, describe the low and high transport rates (Cheng, 2002; Paintal, 1971).

Predictions obtained by using Einstein's bed-load formula are accurate for the bed-load data with moderate transport rates, of which the range, $10^4 < \Psi < 10$, covers all the experimental data used by Einstein (1950) for curve fitting. However, Einstein's formula underestimates the low and high bed-load transport rates that exceed its original domain of validity. Here, the experimental data with low and high bed-load transport

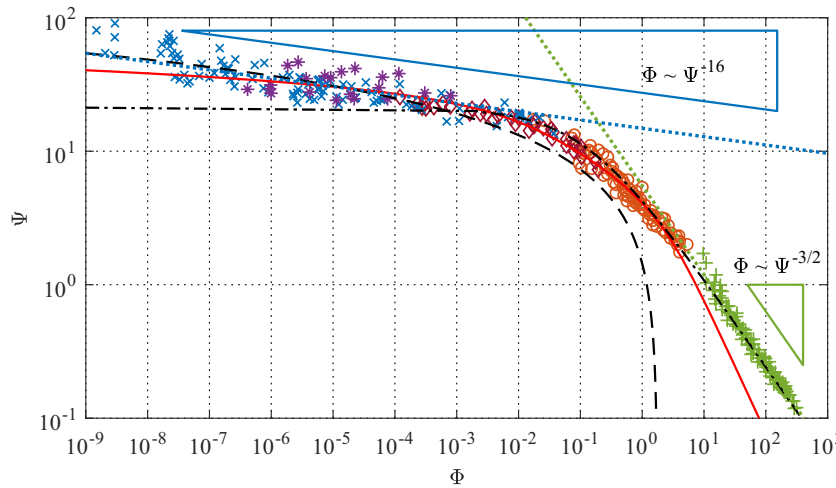

Figure 1. Comparisons between experimental bed-load data (○, Gilbert and Murphy (1914); ◊, Meyer-Peter and Müller (1948); +, Wilson (1966); ×, Paintal (1971); ∗, Taylor and Vanoni (1972), Einstein's bed-load formula (— –, Einstein (1950)), and some empirical formulae (– – –, Einstein (1942); – · – · –, Wilson (1966); ·····, $\Phi \sim \Psi^{-16}$ by Paintal (1971); ·····, $\Phi \sim \Psi^{-1.5}$ by Cheng (2002).

rates were obtained from Paintal (1971) and Wilson (1966), respectively. Paintal (1971) conducted flume tests for 10–20 h to measure very weak bed-load transport rates as low as $\Phi = 10^9$. Wilson (1966) used pressurized conduits to acquire very high bed-load transport data (nylon-sand data are not included in Figure 1).

Figure 1 also shows that some earlier proposed empirical bed-load formulae (Einstein, 1942; Meyer-Peter & Müller, 1948) (the MPM formula was amended by Wilson (1966) for high transport rates) perform better than Einstein's theoretical formula for predicting the low and high transport rates. Einstein (1942) had earlier proposed an empirical exponential function for the low bed-load transport rates as follows:

$$\Phi = C_1 \exp(-k_1 \Psi) \tag{17}$$

where C_1 is a constant, which is related to viscous effects; and k_1 is an exponent ($k_1 > 0$). Under the hydraulically rough flow condition, Einstein (1942) stated that $C_1 = 2.15 \times 0.816 (\approx 1.75)$ and $k_1 = 0.391$. The exponential empirical formula is therefore

$$\Phi = 1.75 \exp(-0.391 \Psi) \tag{18}$$

The good agreement with the data from Paintal (1971) (Figure 1) verifies the validity of the exponential formula (Equation 17) for predicting the low transport rates, viz., $\Phi = 10^{-8} \sim 10^{-4}$. Yet, this formula is woefully inapplicable for higher transport rates, since its prediction of Φ asymptotes toward 1.75 when the applied shear becomes very large or $\Phi \to \infty$.

Meyer-Peter and Müller (1948) suggested a power relationship between Φ and the effective Shields number (i.e., $\Theta - \Theta_C$, in which Θ_C is the critical Shields number) as

$$\Phi = 8\left(\Psi^{-1} - 0.047\right)^{1.5} \tag{19}$$

Later, Wilson (1966) modified the coefficient to 12.1 as

$$\Phi = 12.1\left(\Psi^{-1} - 0.047\right)^{1.5} \tag{20}$$

so that the equation better fits their experimental data with high bed-load transport rates. Figure 1 shows that the MPM-type formulae do not correctly predict data with very low transport rate, because Ψ in the formula is not allowed to be higher than the threshold of the assumed incipient motion of $\Psi = 0.047^{-1}$. Based on recent studies, for example, Lavelle and Mofjeld (1987), it may be surmised that there always exists some particle movement under turbulent flow condition for low shear stresses. For instance, the data of Paintal (1971) were mostly measured with shear stress lower than the presumed critical shear stress.

Moreover, Lavelle and Mofjeld (1987) suggested using power law relationships between Φ and Ψ to evaluate the bed-load transport rates in different small ranges as

$$\Phi = C_2 \Psi^{-k_2} \tag{21}$$

in which C_2 is a constant and k_2 is the exponent ($k_2 > 0$). For example, as shown in Figure 1, in the ranges of the measurements conducted by Paintal (1971) and Wilson (1966), the $\Phi - \Psi$ relation can be, respectively, approximated by using power functions, in which k_2 can be correspondingly treated as a constant.

Paintal (1971) found that if $k_2 = 16$ for the low bed-load transport rates ($\Phi < 10^{-3}$), the data can be fitted very well with the results computed by using the power function

$$\Phi = 5.56 \times 10^{18} \Psi^{-16} \tag{22}$$

For the high transport rates, Chien and Wan (1999) hypothesized that several classical bed-load formulae (Bagnold, 1966; Engelund & Fredsøe, 1976; Meyer-Peter & Müller, 1948; Yalin, 1972) can be reduced to a power relation as $\Phi \sim \Psi^{-1.5}$. Based on this hypothesis, Cheng (2002) modified the MPM formula by fitting the experimental data with high bed-load transport rates to

$$\Phi = 13 \Psi^{-1.5} \tag{23}$$

In summary, the experimental data with very low and high transport rates, which cannot be predicted by using Einstein's bed-load formula, can be represented by some empirical formulae (Equations 18, 20, 22, and 23). The inconsistencies between Einstein's formula and the experimental data are illustrated by comparing the empirically fitted curves and Einstein's curve in the $\log\Phi - \log\Psi$ graph (Figure 1). As shown in the figure, not only do discrepancies between the curves and data exist, but the differences between Einstein's curve and the empirical curves also increase when the bed-load transport rates approach 0 or ∞.

Moreover, although the gradients of Einstein's curve are not strictly constant for very low or high transport rates, they only vary slightly in these regimes. Thus, it is assumed that the gradients of Einstein's curve (Equation 12) when $\Psi \to 0$ and $\Psi \to \infty$ can, respectively, approximate the gradients of $\Psi(\Phi)$ in the ranges of $10^{-9} < \Psi < 10^{-4}$ and $10 < \Psi < 300$. Based on this assumption, the approximate functional forms of Einstein's formula in $10^{-9} < \Psi < 10^{-4}$ and $10 < \Phi < 300$ are calculated, regardless of the values of the parameters in the formula (e.g., A_*, B_*, η_0), and compared with the experimental data in the corresponding ranges. In this case, how the Einstein-assumed probability distribution affects the inconsistencies between the formula and data is elucidated as follows.

According to the definition of probability density function (PDF), a PDF is the derivative of its corresponding CDF,

$$f_{\Psi_*}(\Psi) = \frac{\mathrm{d}F_{\Psi_*}(\Psi)}{\mathrm{d}\Psi} \tag{24}$$

in which $f_{\Psi_*}(\Psi)$ is the PDF of Ψ_*. From the definition of Ψ_*(Equation 13), one can get

$$\frac{\mathrm{d}(1-p)}{\mathrm{d}\Psi} = f_{\Psi_*}(\Psi) \tag{25}$$

and

$$\frac{\mathrm{d}p}{\mathrm{d}\Psi} = -f_{\Psi_*}(\Psi) \tag{26}$$

Thus, the gradient of Einstein's formula in the $\log\Phi - \log\Psi$ graph generally can be deduced from Equations 8 and 13,

$$\frac{\mathrm{d}\ln\Phi}{\mathrm{d}\ln\Psi} = \frac{\mathrm{d}\ln\Phi}{\mathrm{d}p}\frac{\mathrm{d}p}{\mathrm{d}\Psi}\frac{\mathrm{d}\Psi}{\mathrm{d}\ln\Psi} = -\left(\frac{1}{p} + \frac{1}{1-p}\right) f_{\Psi_*}(\Psi)\Psi \tag{27}$$

Furthermore, if the probability distribution in the formula is a folded Gaussian distribution as assumed by Einstein (1950), that is, $\Psi_* = |X|$ (Equation 15), the limits of the gradients of Einstein's formula for $\Psi \to 0$ and $\Psi \to \infty$ can be calculated. This is detailed next.

When $\Psi \to 0$, one can deduce that $\ln\Psi \to -\infty$, and $p \to 1$ from Equation 8. Therefore, the limit of the gradient of Einstein's curve (Equation 27) for $\Phi \to \infty$ is calculated with reference to Equation 13 as follows:

$$\lim_{\Psi\to 0}\frac{\mathrm{d}\ln\Phi}{\mathrm{d}\ln\Psi} = \lim_{\Psi\to 0} -\frac{f_{|X|}(\Psi)}{1-p}\Psi = \lim_{\Psi\to 0} -\frac{f_{|X|}(\Psi)}{F_{|X|}(\Psi)}\Psi = -\Psi \lim_{\Psi\to 0}\frac{f_X(-\Psi)+f_X(\Psi)}{F_X(\Psi)-F_X(-\Psi)} \tag{28}$$

Since CDF is the integral of the corresponding PDF,

$$\lim_{\Psi\to 0} F_X(\Psi) - F_X(-\Psi) = \lim_{\Psi\to 0} \int_{-\Psi}^{\Psi} f_X(t)\mathrm{d}t = \lim_{\Psi\to 0} 2\Psi\left[\frac{f_X(-\Psi) + f_X(\Psi)}{2}\right] \tag{29}$$

Then by substituting Equation 29 into Equation 28, the limit of the gradients of Einstein's curve when $\Psi \to 0$ is calculated as

$$\lim_{\Psi\to 0} \frac{\mathrm{d}\ln\Phi}{\mathrm{d}\ln\Psi} = -1 \tag{30}$$

When $\Psi \to \infty$, $|X|$ becomes indistinguishable from X, viz., the random variable with the corresponding Gaussian distribution ($|X| \to X$). Meanwhile, $p \to 0$ is acquired from Equation 8, so the limit of the gradient of Einstein's curve when $\Psi \to \infty$ is also calculated from Equation 27 as follows:

$$\lim_{\Psi\to\infty} \frac{\mathrm{d}\ln\Phi}{\mathrm{d}\ln\Psi} = \lim_{\Psi\to\infty} -\frac{f_X(-\Psi)}{p}\Psi = \lim_{\Psi\to\infty} -\frac{f_X(\Psi)}{1 - F_X(\Psi)}\Psi = -\Psi \lim_{\Psi\to\infty} H_X(\Psi) \tag{31}$$

in which $H_X(\Psi) = f_X(\Psi) / [1 - F_X(\Psi)]$ is the so-called hazard function, which is commonly used in engineering studies (Forbes et al., 2011). Thus, according to the definition of X (Equation 16), one can derive that

$$\lim_{\Psi\to\infty} H_X(\Psi) = \lim_{\Psi\to\infty} \frac{f_X(\Psi)}{1 - F_X(\Psi)} = \lim_{\Psi\to\infty} \frac{f_X^{'}(\Psi)}{-f_X(\Psi)} = \frac{\Psi - \mu}{\sigma^2} = B_*^2\Psi - B_*\eta_0^{-1} \tag{32}$$

Therefore, the limit of the gradient of Einstein's curve when $\Psi \to \infty$ is

$$\lim_{\Psi\to\infty} \frac{\mathrm{d}\ln\Phi}{\mathrm{d}\ln\Psi} = -B_*^2\Psi^2 + B_*\eta_0^{-1}\Psi \tag{33}$$

In brief, the gradient of the curve of Einstein's formula in the plot of $\log\Phi - \log\Psi$ is close to -1 for the high bed-load transport rates ($10 < \Phi < 300$) and the formula can be approximated by a quadratic function, that is, $-B_*^2\Psi^2 + B_*\eta_0^{-1}\Psi$, for the low bed-load transport rates ($10^{-9} < \Phi < 10^{-4}$). According to the foregoing calculations, these arguments are closely associated with the folded Gaussian distribution assumed by Einstein (1950). In the following, the derived the gradients of Einstein's formula at the limits are compared with the gradients of the empirical formulae that represent the trends of the experimental data outside the range of validity of Einstein's formula.

In the regime of high bed-load transport rate, the gradients of both the empirical power function proposed by Cheng (2002) (Equation 23) and the MPM-type formulae from Meyer-Peter and Müller (1948) and Wilson (1966) (Equations 19 and 20) are -1.5 in the plot of $\log\Phi - \log\Psi$. Thus, the disagreement in predicting high bed-load transport rates is inevitable for Einstein's formula, whose gradients approach -1 in this regime.

In the regime of low bed-load transport rate, the gradient of the power function (Equation 22) proposed by Paintal (1971) equals -16, and the gradient of the exponential formula by Einstein (1942) can be calculated from Equation 18 as 0.391Ψ. However, it is not easy to distinguish in Figure 1 whether the scattered data with $\Phi < 10^{-4}$ is more compatible with a gradient that is, constant or decreasing linearly with Ψ. Despite that, it is apparent that Einstein's formula (Equation 12) has underestimated them. Moreover, the gradient of Einstein's curve at the limit, which has the form of a quadratic function (Equation 33), must increasingly deviate from the trend of data when $\Psi \to \infty$. Thus, the disagreement in predicting the low bed-load transport rate is also inevitable for Einstein's formula.

Similar work that calculates the limiting forms of Einstein's original formula has been done by Yalin (1972), but the present analysis further shows the relation between the gradients at the limits and the presumed probability distribution. Since the numerical values of B_* and η_0 are undetermined in the above calculations, the incompatibility of Einstein's original formula with very low or high bed-load transport rates cannot be alleviated by recalibrating the parameters of the probability distribution. In conclusion, the incompatibility is inherent in the type of probability distribution assumed by Einstein (1950), that is, the folded Gaussian distribution.

2.3. Comparison of the PDF of Ψ_*

To obtain a more reasonable probability distribution, a decreasing and continuous $p(\Psi)$ relation should be first developed, and then an appropriate distribution function $F_{\Psi_*}(\Psi)$ should be fitted to $1-p(\Psi)$ (according to Equation 13). The data fitting, however, cannot be achieved by using a general method, such as linear regression, because the data points in the plot of $\Phi-\Psi$ are scattered and the specific functional form of $F_{\Psi_*}(\Psi)$ is undetermined. Therefore, two techniques are introduced to explore the type of probability distribution.

First, the experimental data used for the curve fit should not cover the whole measurable range. Instead, only the data with very low and high transport rates are considered. Moreover, Gaussian distribution is known to be defective in describing many natural events under extreme conditions. For instance, Bramwell et al. (1998) found that the high-magnitude velocity fluctuations in turbulent flows are better described by a non-Gaussian distribution. Valyrakis et al. (2011) found that the frequencies of the impulses with different magnitudes induced by the extreme near-bed turbulent events are better fitted by an exponential distribution. Thus, it is deduced that the accuracy in describing the probability of extreme values (corresponding to $p(\Psi)$ when Ψ is extremely small or large) can be investigated to determine which type of non-Gaussian probability distribution can be better fitted.

Second, the trends of the relation of $\Phi-\Psi$ when $\Phi\to 0$ and $\Phi\to\infty$ are, respectively, anticipated from the data trends when Φ is very low and high. They are used to engender the gradients of $p(\Psi)$ when $p\to 0$ and $p\to 1$. This anticipation is applicable because Paintal (1971) and Wilson (1966) had measured numerous experimental data that are almost at the extreme levels. Therefore, one can assume that the trends fitted to these data sets can anticipate the possible trends of the data in the extended range. With this consideration, $F_{\Psi_*}(\Psi)$ is not directly fitted to $1-p(\Psi)$, but their gradients at the limits are compared. This is because the distribution functions of commonly used probability distributions are different, but their gradients when $p\to 0$ and $p\to 1$ can usually be categorized into simple functions (e.g., power function, exponential function). An appropriate distribution of Ψ_* may be obtained by fitting the gradients of $F_{\Psi_*}(\Psi)$ at the limits to those of $1-p(\Psi)$. However, the gradients of different $F_{\Psi_*}(\Psi)$ at the limits are not convenient to be illustrated and compared in the CDF plots. Thus, the derivatives of $1-p(\Psi)$ are further calculated to be compared with the PDF plots of different probability distributions. In this case, the gradients of $1-p(\Psi)$ at the limits are used to fit the left and right tails of the PDF of the probability distribution to replace $|X|$.

Yet, the differences in the tails of PDFs, sometimes, are still hardly distinguishable on a normal plot of PDF, because the common PDF similarly approaches zero when the random variable approaches extreme values. Bagnold (1983) suggested using log-scale plots of PDF to describe the asymptotic trends of the tails of PDF, and similar treatments are also adopted by many recent studies, for example, Ancey et al. (2006) and Bramwell et al. (1998). With this approach, the folded Gaussian distribution $|X|$ and a probability distribution that is, best fitted to the experimental data are compared through the plots of their PDFs. The comparison is presented in two ways: (a) visually comparing the differences between the PDF plots of $|X|$ and the best fit probability distribution; and (b) calculating the different gradients at the limits of these PDFs.

The analyses based on the comparisons between the PDFs conducted in this section are the preliminary work before determining the specific probability distribution of Ψ_* in Section 3. The best fit probability distribution used here may not have a complete and explicit distribution function, and thus it cannot be used to engender a bed-load formula. Nonetheless, the comparisons are expected to reveal the required limiting behavior of the probability distribution to replace $|X|$.

As shown in the schematic diagram (Figure 2), the comparison of PDFs can be transformed from the foregoing comparison of $\Phi(\Psi)$ in Section 2.2. The relationships between the functions involved in the transformation, that is, PDF of Ψ_*, $p(\Psi)$, and $\Phi(\Psi)$, are illustrated by the black boxes and arrows in Figure 2. As for Einstein's formula, the comparisons based on $\Phi(\Psi)$ and PDF of Ψ_* are mathematically equivalent, because the functions can be mutually transformed (using Equations 8, 13, and 24).

For the best fit probability distribution obtained from the experimental data, however, data fitting is needed because the scattered $\Phi(\Psi)$ data cannot be plotted on a graph of PDF. In order to obtain the PDF from $\Phi(\Psi)$, according to Equation 13, $1-p(\Psi)$ is compared to a distribution function (CDF), so it has to be continuous and non-decreasing. Thus, as shown by the red dashed arrow and circles in Figure 2, the experimental data

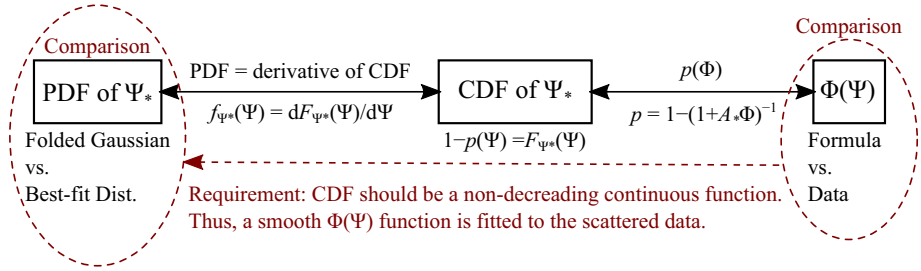

Figure 2. Schematic diagram of the relationship of two approaches for comparing Einstein's bed-load formula and experimental data. Left circle: comparison of PDFs of $|X|$ and the best fit probability distribution; Right circle: comparison of $\Phi(\Psi)$ against the $\Phi - \Psi$ data.

are first used to fit a smooth function $\Phi(\Psi)$. Then, a best fit PDF is deduced from the $\Phi(\Psi)$ function to be compared with the PDF of $|X|$.

First, a locally estimated scatterplot smoothing (LOESS) method (Garimella, 2017) is used to fit a smooth $\Phi(\Psi)$ function to the data in the plot of $\log\Psi - \log\Phi$. The method calculates a weight parameter for every data point when fitting the smooth curve at a certain location:

$$w(\Psi) = \left(1 - \left|\log\Psi - \log\Psi_0\right|^3\right)^3 \tag{34}$$

in which $w(\Psi)$ is the weight parameter that depends on the x-direction distance in the $\log\Psi - \log\Phi$ plot between the curve-fitting point at $x = \Psi_0$ and the data point at $x = \Psi$. With the weight parameters, the LOESS fitting is conducted at every point on the fitted curve by applying a weighted regression to the 20% most neighboring data. In this way, a smooth $\Phi(\Psi)$ function that is, optimally fitted to all the data in the $\log\Psi - \log\Phi$ plot is obtained as shown in Figure 3a. In the following analysis, this function obtained by using the LOESS fitting method is denoted as the best fit $\Phi(\Psi)$ function. Figure 3a shows the comparison between the best fit $\Phi(\Psi)$ and the experimental data. By assuming $A_* = 43.50$ (following Einstein (1950)), the best fit $\Phi(\Psi)$ can be further transferred to a best fit $p(\Phi)$ (using Equation 8). Figure 3b shows the best fit distribution function (CDF) of Ψ_* obtained from the trends of data, that is, $1 - p(\Psi)$, which is also compared with the experimental data.

Next, the best fit PDF of Ψ_* is obtained from the derivative of $1 - p(\Psi)$ (Equation 25), that is, the CDF in Figure 3b. The result is presented in Figure 4a, which shows a positive-support bell-curve PDF (denoted as open circles). Besides, the PDF of $|X|$, that is, the folded Gaussian distribution in Einstein's formula (denoted

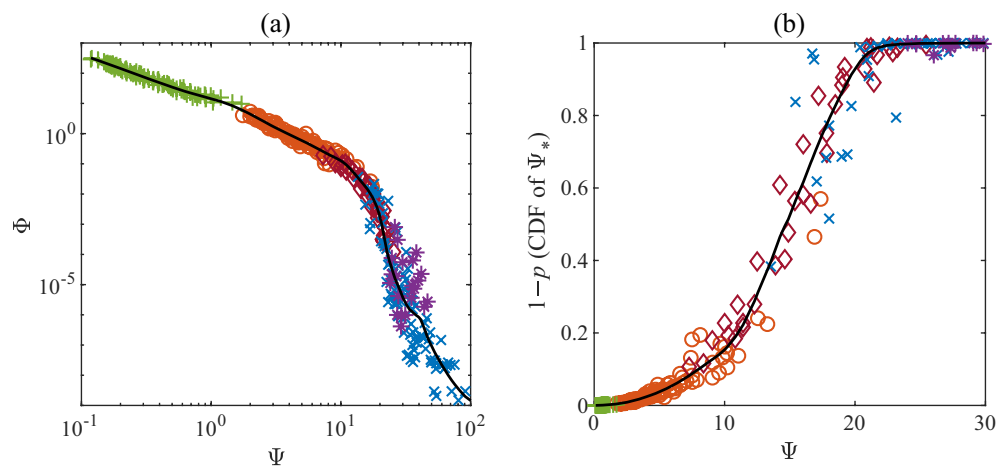

Figure 3. Transfer from (a) $\Phi(\Psi)$ function (——) that is, optimally fitted to the data (◦, Gilbert and Murphy (1914); ◊, Meyer-Peter and Müller (1948); +, Wilson (1966); ×, Paintal (1971); ∗, Taylor and Vanoni (1972)) in the $\log\Psi - \log\Phi$ plot to (b) the best fit CDF of Ψ_*.

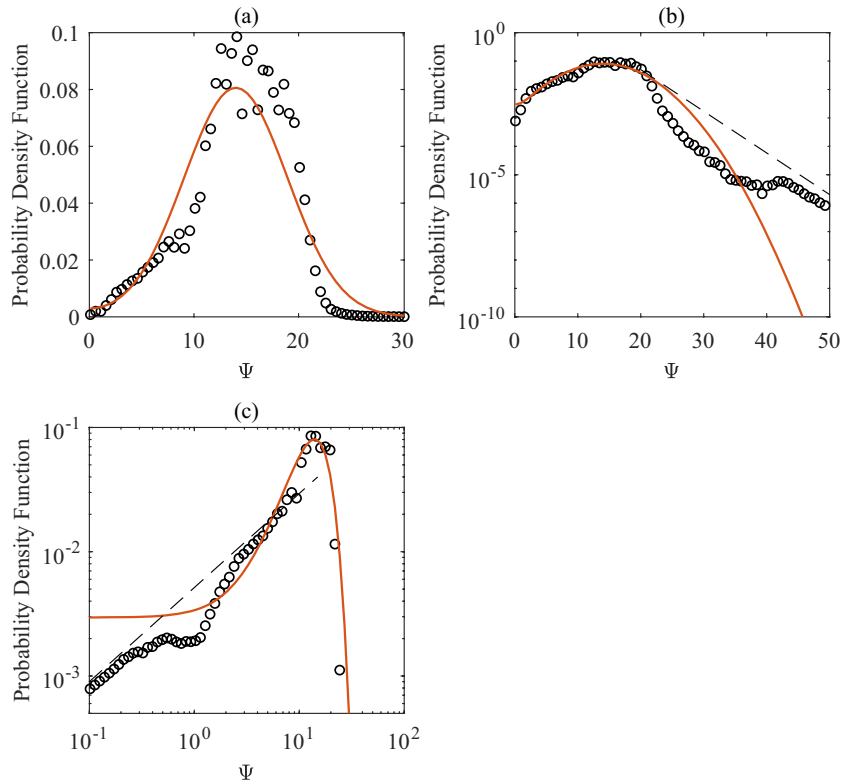

Figure 4. Comparison between the PDF of Einstein's probability distribution $|X|$ (— –, (Einstein 1950)) and the best fit PDF (∘∘∘), plotted when (a) coordinates are in linear scale (b) *y*-coordinate is in log-scale; (c) both *x*-coordinate and *y*-coordinate are in log-scale. Asymptotes of the tails of the PDF are presented as dashed lines (– – –).

as red line), is superimposed for comparison. As expected, in the normal (linear) plot of PDFs (Figure 4a), the differences between the tails of the two PDFs are not significant enough to be distinguishable.

In accordance with the suggestion of Bagnold (1983), the differences, however, are more clearly shown if the *y*-coordinate is plotted in log-scale (Figure 4b), or both coordinates are plotted in log-scale (Figure 4c). When $\Psi \to \infty$, the PDF of $|X|$ in Figure 4b has a significant downward curvature, but the best fit PDF has an approximately straight-line trend. When $\Psi \to 0$, Figure 4c shows that the two PDFs also are incompatible. The PDF of $|X|$ approaches a horizontal line in Figure 4c, while the trend of the best fit PDF clearly is non-horizontal. Therefore, the comparisons of the PDFs in Figure 4 reveal that $|X|$ fails to describe the limiting behavior of the best fit probability distribution that is deduced from the experimental data. Besides, the comparison shows that the disagreement between Einstein's formula and the trends of data is implied in the limiting behavior of $|X|$.

Accordingly, the PDF of the probability distribution used to replace $|X|$ should have similar tails like those of the best fit PDF shown in Figures 4b and 4c, when $\Psi \to \infty$ and $\Psi \to 0$, respectively. It is reasonable to assume that the right and left tails of the best fit PDF, respectively, have asymptotes (dashed lines) in Figures 4b and 4c that are straight lines with undetermined gradients. With these assumptions, although the best fit PDF cannot be explicitly expressed as a function, the limiting behaviors of the best fit PDF can be approximately described by using simple functions. Thus, the limiting forms of the best fit PDF are approximated, respectively, as a power function when $\Psi \to 0$ and an exponential function when $\Psi \to \infty$.

Then, to specifically determine the probability distribution to replace $|X|$, the foregoing techniques that suggest fitting the limiting behavior of the probability distribution to the trends of data at the limits are applied. Instead of fitting to all the data by using the LOESS method, the data with the very low and high transport rates are fitted by using simple functions (e.g., linear, power, exponential functions). The fitted functions are

used to anticipate the trends of the data at the limits when the bed-load transport rate approaches 0 and ∞, thus they are required to match the approximate limiting forms of the best fit PDF.

Hence, calculations are conducted in the following to show if the limiting behavior of the best fit probability distribution (through its PDF) can be represented by Equation 1 an exponential relationship $\Phi = C_1 \exp(-k_1\Psi)$ (Equation 17) (Einstein, 1942) for very small transport rates; and (2) a power law relationship $\Phi = C_2\Psi^{-k_2}$ (Equation 21) (Lavelle & Mofjeld, 1987) for very large transport rates. Besides, the gradients of the PDF of the folded Gaussian distribution at the limits in Figures 4b and 4c are also calculated for comparison. In the following calculations, Ψ_* is denoted as $\hat{\Psi}$ to represent the probability distribution that renders $\Phi(\Psi)$ to have the required trends at the limits.

First, considering the limiting form of the PDF when $\Psi \to \infty$, the folded Gaussian distribution $|X|$ becomes indistinguishable with the corresponding Gaussian distribution $X \sim \mathcal{N}(\mu,\sigma)$ (Equation 16) when $\Psi\mu/\sigma^2$ is large enough (error is less than 1% if $\Psi\mu/\sigma^2 > 2.3$). Thus, when $\Psi \to \infty$, the PDF can be approximated as

$$\lim_{\Psi\to\infty} f_{|X|}(\Psi) \approx f_X(\Psi) = \frac{1}{\sigma\sqrt{2\pi}}\exp\left[-\frac{1}{2}\left(\frac{\Psi-\mu}{\sigma}\right)^2\right] \tag{35}$$

Based on this presupposition, the curve of the PDF of $|X|$ has the limiting form as a parabola when $\Psi \to \infty$ if the y-coordinate is in the logarithmic scale (as Figure 4b) because

$$\lim_{\Psi\to\infty} \ln\left[f_{|X|}(\Psi)\right] \approx -\frac{1}{2}\left(\frac{\Psi-\mu}{\sigma}\right)^2 - \ln\sigma - \frac{1}{2}\ln 2\pi \tag{36}$$

On the other hand, the gradients of the PDF curve of $\hat{\Psi}$ in a plot with log-scale y-coordinate is calculated as

$$\frac{\mathrm{d}\ln f_{\hat{\Psi}}(\Psi)}{\mathrm{d}\Psi} = \mathrm{d}\ln\left[\frac{\mathrm{d}(1-p)}{\mathrm{d}\Psi}\right]/\mathrm{d}\Psi = \mathrm{d}\ln\left[\frac{\mathrm{d}(1+A_*\Phi)^{-1}}{\mathrm{d}\Psi}\right]/\mathrm{d}\Psi \tag{37}$$

If the data with very low bed-load transport rates are approximated by $\Phi = C_1\exp(-k_1\Psi)$ (Equation 17), the limit of the gradient of the PDF of $\hat{\Psi}$ is nearly a constant when $\Psi \to \infty$:

$$\lim_{\Psi\to\infty}\frac{\mathrm{d}\ln f_{\hat{\Psi}}(\Psi)}{\mathrm{d}\Psi} = \lim_{\Psi\to\infty} -k_1 + \frac{2k_1A_*C_1\exp(-k_1\Psi)}{1+A_*C_1\exp(-k_1\Psi)} = -k_1 \tag{38}$$

Second, the limiting form of the PDF when $\Psi \to 0$ is calculated. The PDF of $|X|$ is

$$f_{|X|}(\Psi) = \sqrt{\frac{2}{\pi\sigma^2}}\exp\left(-\frac{\Psi^2+\mu^2}{2\sigma^2}\right)\cosh\left(\frac{\mu\Psi}{\sigma^2}\right) \tag{39}$$

When $\Psi \to 0$, the limit of the gradients of $f_{|X|}(\Psi)$ in a double-log coordinate system (as Figure 4c) is

$$\lim_{\Psi\to 0}\frac{\mathrm{d}\ln f_{|X|}(\Psi)}{\mathrm{d}\ln\Psi} = \lim_{\Psi\to 0}\left[-\frac{\Psi}{\sigma^2} + \frac{\mu}{\sigma^2}\tanh\left(\frac{\mu\Psi}{\sigma^2}\right)\right]\Psi = 0 \tag{40}$$

The curve of the PDF of $|X|$ asymptotically approaches a horizontal line when $\Psi \to 0$.

The gradient of the PDF of $\hat{\Psi}$ in the double-log coordinate system (as Figure 4c) can be obtained by utilizing Equation 21 as

$$\frac{\mathrm{d}\ln f_{\hat{\Psi}}(\Psi)}{\mathrm{d}\ln\Psi} = \mathrm{d}\ln\left[\frac{\mathrm{d}(1-p)}{\mathrm{d}\Psi}\right]/\mathrm{d}\ln\Psi = \left\{\mathrm{d}\ln\left[\frac{\mathrm{d}(1+A_*\Phi)^{-1}}{\mathrm{d}\Psi}\right]/\mathrm{d}\Psi\right\}\Psi \tag{41}$$

If $\Phi = C_2\Psi^{-k_2}$ (Equation 21) is used to fit the data with very high bed-load transport rates, the gradient of the PDF curve approaches a constant when $\Psi \to 0$

$$\lim_{\Psi\to 0}\frac{\mathrm{d}\ln f_{\hat{\Psi}}(\Psi)}{\mathrm{d}\ln\Psi} = \lim_{\Psi\to 0} -(k_2+1) + \frac{2k_2A_*C_2\Psi^{-k_2}}{1+A_*C_2\Psi^{-k_2}} = k_2 - 1 \tag{42}$$

in which $k_2 > 1$.

As a result, the calculation of the gradients of the PDF of $|X|$ at the limits verifies the foregoing observations on $|X|$'s PDF curves in Figures 4b and 4c. The gradients of the PDF of $\hat{\Psi}$ at the limits are proven to be constant in the corresponding coordinate systems (as in Figures 4b and 4c). The differences between the

calculated gradients of the PDFs show again the limiting behaviors of the Einstein-assumed probability distribution, that is, $|X|$, is inappropriate for fitting Einstein's formula to the experimental data.

Furthermore, the results show that the PDF of $\hat{\Psi}$ has the same limiting behavior as that indicated by the straight-line asymptotes assumed in Figures 4b and 4c, which approximate the tails of the best fit PDF. Therefore, if an exponential function and a power function can be, respectively, well fitted to the $\Phi - \Psi$ data with very small and large transport rates, a probability distribution whose PDF approaches an exponential function when $\Psi \to \infty$ and a power function when $\Psi \to 0$ (viz. fit to the data) can be found to optimally match the best fit probability distribution (whose PDF is shown in Figure 4). Moreover, because the tails of the PDF follow simple functional law, it is expected a commonly used probability distribution with the matched tails may be found to replace $|X|$ in a modified Einstein-type formula, which is conducted next in Section 3.

3. Modification of the Probability Distribution

3.1. Determination of the Probability Distribution

The modification of the probability distribution in Einstein's formula takes two steps. First, a common type of probability distribution whose limiting behavior matches the tails of the PDF of $\hat{\Psi}$ is needed. The limiting form of the tails follows an exponential law when $\Psi \to \infty$ and a power law when $\Psi \to 0$. With this approach, the type of probability distribution used to replace $|X|$ is first determined.

Second, the foregoing proposed functions, that is, exponential function and power function, are, respectively, fitted to the experimental data with low and high transport rates. According to the trends of data at the limits anticipated by the fitted functions, the limiting forms of the probability distribution to replace $|X|$ can be specified. In most cases, once the tails of a classic type of probability distribution are confirmed, its distribution function is determined.

To obtain a classic type of positive-support probability distribution whose PDF has similar tails like those of $\hat{\Psi}$, the generalized Gamma distribution from Stacy (1962) is investigated. This is because the generalized Gamma distribution represents a family of distributions that covers a wide range of commonly used probability distributions, such as the log-normal distribution and the Weibull distribution (Crooks, 2010). Besides, the positive even powers and modulus of a centered Gaussian distribution also are special cases of generalized Gamma distribution (Block & Rao, 1974). Therefore, it is assumed that $\Psi_* = G^+$ where

$$G^+ \sim \mathcal{G}^+(k,\theta,\beta) \tag{43}$$

in which k, θ, and β are the parameters of a generalized Gamma distribution $\mathcal{G}^+$. Following the general notations (Crooks, 2010), the PDF of the generalized Gamma distribution is

$$f_{G^+}(\Psi) = \frac{\beta}{\theta\Gamma(k)}\left(\frac{\Psi}{\theta}\right)^{k\beta-1}\exp\left[-\left(\frac{\Psi}{\theta}\right)^{\beta}\right] \tag{44}$$

in which $\Gamma(k)$ is the standard Gamma function

$$\Gamma(k) = \int_0^\infty t^{k-1}\exp(-t)\mathrm{d}t \tag{45}$$

Hence, the logarithm of the PDF is

$$\ln f_{G^+}(\Psi) = (k\beta-1)\ln\left(\frac{\Psi}{\theta}\right) - \left(\frac{\Psi}{\theta}\right)^{\beta} + \ln\left[\frac{\beta}{\theta\Gamma(k)}\right] \tag{46}$$

The limiting forms of $\ln f_{\Psi_*}(\Psi)$ are

$$\lim_{\Psi\to\infty}\ln f_{G^+}(\Psi) = -\left(\frac{\Psi}{\theta}\right)^{\beta} \tag{47}$$

$$\lim_{\Psi\to 0}\ln f_{G^+}(\Psi) = (k\beta-1)\ln\left(\frac{\Psi}{\theta}\right) \tag{48}$$

According to the gradients of the PDF of $\hat{\Psi}$ at the limits calculated in Section 2.3 (Equations 38 and 42), the limiting forms of the logarithm of the PDF of $\hat{\Psi}$ are

$$\lim_{\Psi\to\infty} \ln f_{\hat{\Psi}}(\Psi) \sim \Psi \tag{49}$$

$$\lim_{\Psi\to 0} \ln f_{\hat{\Psi}}(\Psi) \sim \ln\Psi \tag{50}$$

Comparing with the limiting forms of the logarithm of the best fit PDFs when $\Psi \to \infty$ and $\Psi \to 0$ (Figures 4b and 4c), one obtains the requirements of the parameters: $\beta = 1$, $k > 1$, and $\theta > 0$. If the probability distribution of G^+ meets these criteria, the tails of its PDF have the similar trends as those of the best fit PDF. It is known that, when $\beta = 1$, the generalized Gamma distribution $\mathcal{G}^+(k,\theta,\beta)$ degrades into the Gamma distribution $\mathcal{G}(k,\theta)$. It is hence assumed that Ψ_* has a Gamma distribution, denoted as $\Psi_* = G$ where

$$G \sim \mathcal{G}(k,\theta) \tag{51}$$

in which k is the shape parameter and θ is the scale parameter.

If Einstein's probability distribution is revised as a Gamma distribution (replacing $|X|$ by G), three parameters in the modified Einstein-type formula, viz., A_*, k, and θ, need to be calibrated by using the experimental data. The determination of their values, as expected, does not need to fit all the experimental data but only the data with low and high transport rates (Paintal, 1971; Wilson, 1966).

Knowing that the PDF of a Gamma distribution is

$$f_G(\Psi) = \frac{1}{\Gamma(k)\theta^k}\Psi^{k-1}\exp(\Psi/\theta) \tag{52}$$

where the parameters of the Gamma distribution, k and θ, are calibrated by fitting the limiting forms of the PDF of G. Compared with the limiting forms of the PDF of $\hat{\Psi}$, which have been described by Equations 38 and 42, k and θ are determined as

$$\lim_{\Psi\to\infty} \frac{\mathrm{d}\ln f_G(\Psi)}{\mathrm{d}\Psi} = -\frac{1}{\theta} = \lim_{\Psi\to\infty} \frac{\mathrm{d}\ln f_{\hat{\Psi}}(\Psi)}{\mathrm{d}\Psi} = -k_1 \tag{53}$$

$$\lim_{\Psi\to 0} \frac{\mathrm{d}\ln f_G(\Psi)}{\mathrm{d}\ln\Psi} = k - 1 = \lim_{\Psi\to 0} \frac{\mathrm{d}\ln f_{\hat{\Psi}}(\Psi)}{\mathrm{d}\ln\Psi} = k_2 - 1 \tag{54}$$

According to the analysis in Section 2.3, calibrating k and θ by fitting the Gamma distribution is hereby transferred to fitting two simple functions (Equations 17 and 21) to the experimental data.

Noticing that the empirical formula from Einstein (1942) is an exponential function and one of the formulae proposed by Cheng (2002) is a power function, there is no need to fit the functions to the corresponding data again to determine k_1 and k_2. It has been shown in Figure 1 that the exponential formula from Einstein (1942) (Equation 18) is in good agreement with the trend of the data from Paintal (1971) (visually verified) and the power formula from Cheng (2002) (Equation 23) optimally matches the data from Wilson (1966) (best fitted in the study by Cheng (2002)). Thus, the empirical formulae from Einstein (1942) and Cheng (2002) can be regarded as, respectively, good fittings of the trends of data with very low and high transport rates. Thus, the values of the parameters of G are calibrated as $k = k_2 = 1.5$ (or 3/2); and $\theta = 1/k_1 = 1/0.391$ (or 2.56).

3.2. Determination of the Formula

After the Gamma distribution is determined, only the value of A_* needs to be calibrated. Figure 5 displays the different best fit PDF derived from the experimental data by assuming $A_* = 0.1$, 1, and 10. Figure 5b shows that the right tail of the best fit PDF moves upwards when A_* increases from 0.1 to 10, while Figure 5c shows that the left tail moves downwards correspondingly. It is observed that the above-determined Gamma distribution PDF curve appears between the best fitted PDFs with, respectively, $A_* = 0.1$ and $A_* = 1$.

Therefore, as shown in Figure 6, by applying trial-and-error at the precision of 0.01 in the range between 0.1 and 1, the value of A_* that renders the least square of sum for the residuals between $\log\Phi$ of the data with very low and high transport rates (Paintal, 1971; Wilson, 1966) and the formula improved with Gamma distribution (using Equation 7) is determined as 0.45. The fitted formula is shown as the solid curve in Figure 6. Figure 6 also shows the empirical formulae (Cheng, 2002; Einstein, 1942) that are used to calibrate

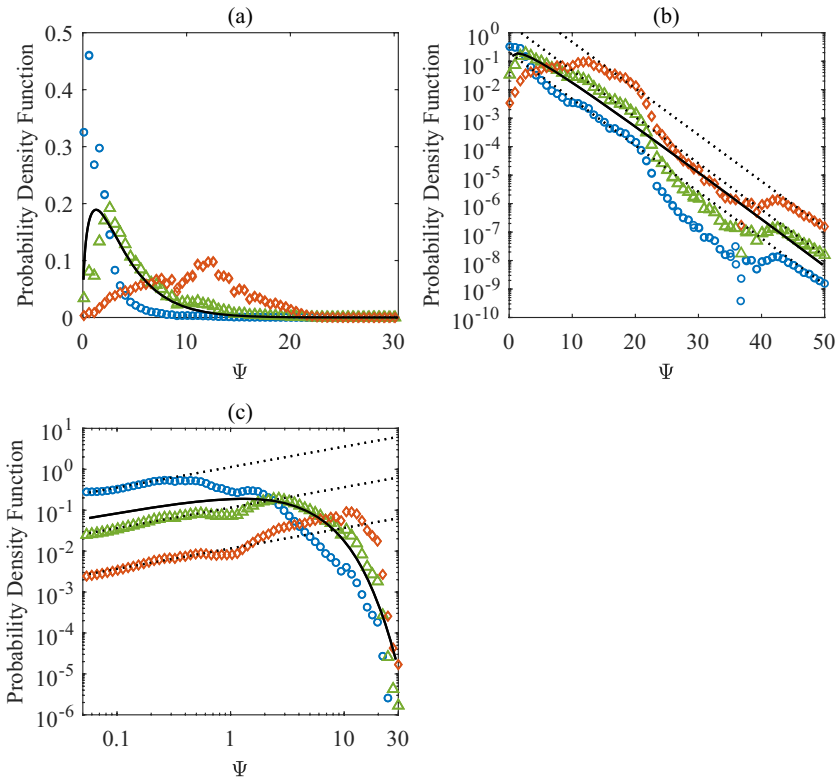

Figure 5. The best fit PDF plotted by, respectively, assuming $A_* = 0.1$ (○○○), 1 (△△△), 10 (◇◇◇), and the PDF of the Gamma distribution (——) that fits the trends of the data with low and high transport rates at the limits. (a) Linear coordinates; (b) The *y*-coordinate is in log-scale; (c) The *x*-coordinate and *y*-coordinate are in log-scale. Asymptotes of the tails of the best fit PDFs are presented as dotted lines (·····).

the Gamma distribution. It is noted that, after A_* is determined, the curve of the formula is optimally fitted to all the data points, and has a gap from the exponential formula proposed by Einstein (1942). It reveals that when fitting the probability distribution, only the trends of data are utilized, regardless of the absolute locations of the data points. This feature also has been indicated in Equations 38 and 42, where only k_1 and

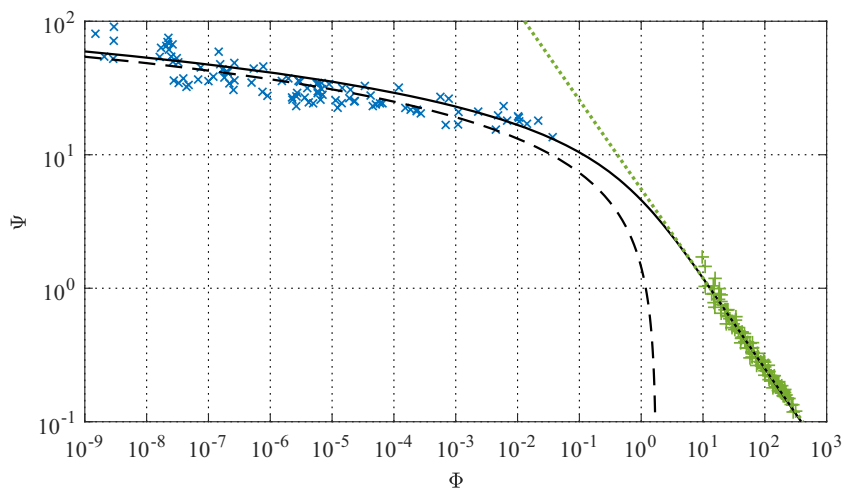

Figure 6. The data set (+, Wilson (1966); ×, Paintal (1971)) and empirical formulae (– – –, Einstein (1942); ·····, Cheng (2002)) that are used to calibrate the parameters (k, θ, and A_*) in the formula modified by using Gamma distribution (——).

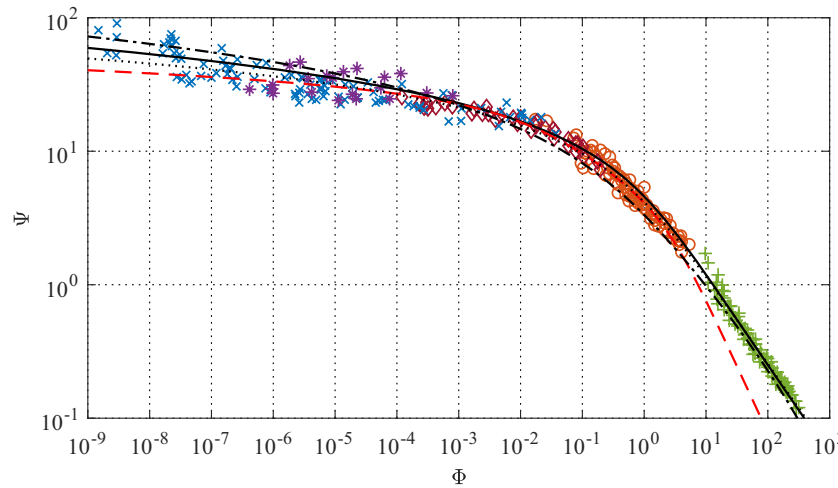

Figure 7. Comparison between the present formula improved with Gamma distribution (——, this study), the formula proposed by Einstein (1950) (– – –), the formula proposed by Armanini et al. (2015) (– · – · –), the empirical formula from Cheng (2002) (·····), and the experimental data (○, Gilbert and Murphy (1914); ◊, Meyer-Peter and Müller (1948); +, Wilson (1966); ×, Paintal (1971); ∗, Taylor and Vanoni (1972)).

k_2 are used to described the tails of PDF (without C_1 and C_2). In summary, only partial information of the data set is used to determine the probability distribution and calibrate the parameters in the modified Einstein-type formula.

Consequently, by regarding $p(\Psi)$ as the complementary distribution function of the Gamma distribution (using Equation 13) and determining $\Phi(p)$ by using Equation 8 with $A_* = 0.45$, the improved bed-load formula is derived as

$$\Phi = \frac{1}{0.45}\left\{\left[\frac{\gamma(3/2, 0.391\Psi)}{\Gamma(3/2)}\right]^{-1} - 1\right\} \tag{55}$$

in which the lower incomplete gamma function $\gamma(k,x)$ is defined as

$$\gamma(k,x) = \int_0^x t^{k-1}\exp(-t)\mathrm{d}t \tag{56}$$

Since $k = 3/2, \Gamma(3/2) = \sqrt{\pi}/2$, the modified bed-load formula is

$$\Phi = \frac{1}{0.45}\left[\frac{\sqrt{\pi}}{2}\left(\int_0^{0.391\Psi}\sqrt{t}\exp(-t)\mathrm{d}t\right)^{-1} - 1\right] \tag{57}$$

Moreover, if the lower incomplete gamma function is expressed in terms of the error function $\mathrm{erf}(x)$

$$\gamma\left(\frac{3}{2}, x\right) = \frac{\sqrt{\pi}}{2}\mathrm{erf}(\sqrt{x}) - \sqrt{x}\exp(-x) \tag{58}$$

in which

$$\mathrm{erf}(x) = \frac{\sqrt{\pi}}{2}\int_0^x \exp(-t^2)\mathrm{d}t \tag{59}$$

the modified bed-load formula can also be written as

$$\Phi = \left[0.45\mathrm{erf}(0.625\sqrt{\Psi}) - 0.318\sqrt{\Psi}\exp(-0.391\Psi)\right]^{-1} - 2.22 \tag{60}$$

The comparisons between the present formula improved by the Gamma distribution $G(k = 3/2, \theta = 1/0.391)$, the experimental data (Gilbert & Murphy, 1914; Meyer-Peter & Müller, 1948; Paintal, 1971; Taylor & Vanoni, 1972; Wilson, 1966), Einstein's original formula (Einstein, 1950), and the empirical formula from Cheng (2002) are presented in Figure 7. Compared with Einstein's original formula, the match between the prediction of the modified bed-load formula and experimental results are significantly improved. The curve of the present formula is very close to that of the formula proposed by Cheng (2002) and nearly coincides with it in the high transport regime. Thus, this formula can accurately evaluate the bed-load transport rates

in $10^{-9} < \Phi < 300$. Besides, the present modified bed-load formula is in good agreement with the trends of the experimental data with very low and high bed-load transport rates. Therefore, the weakness of Einstein's formula, that is, that error of the prediction increases when the bed-load transport rates approach extremely low or high level, is also overcome with the modification of the probability distribution.

The formula proposed by Armanini et al. (2015), that is,

$$\Phi = \frac{25(2+\Psi)}{2\Psi(1+4\Psi)}\exp\left[-\frac{1}{2}\left(\frac{\Psi}{2}-1\right)\right] \tag{61}$$

in which the parameters in the corresponding functions in Table 1 were calibrated as $A_u = 0.25$, $a = 0.5$, $K_1 = 100$, $K_2 = 4$, $B_* = 0.25$, and $\eta_0 = 2$, is also compared with the present formula in Figure 7. It is found that both formulae predict the experiment data with low and high transport rates better than Einstein's formula, but the formula from Armanini et al. (2015) appears to underestimate the bed-load transport rates in $\Phi > 10^{-3}$. While the present study retains the form of $\Phi(p)$ assumed by Einstein (1950), the study of Armanini et al. (2015) proposes a different form of $\Phi(p)$. Hence, one may surmise that the Gamma distribution has very flexible functional form and can be well fitted to the data when $\Phi(p)$ is assumed to have different forms. Although it is still uncertain which Gamma distribution describes the practical sediment entrainment more accurately, a possible physical meaning of the present Gamma distribution is discussed in the following section.

4. Discussion

The present study revises the probability distribution assumed by Einstein (1950) based on data fitting, but retains the remaining functional form of the bed-load formula (i.e., $\Phi(p)$) following Einstein's original assumptions. Thus, the physical meaning of p should still be the probability of sediment entrainment. However, p is not likely to be determined by $F_L > W'$ because Diplas et al. (2008) has shown that the instantaneous peak hydrodynamic force is not a sufficient to determine sediment entrainment.

Nevertheless, the present study does not assume the criterion of sediment entrainment before data fitting. Similarly, Armanini et al. (2015) presupposed their probability distribution based on the statistics of moving particles measured by Ancey et al. (2006), which, however, did not include the measurements of hydrodynamic forces. Thus, the underlying physics of using the Gamma distributions to evaluate sediment entrainment need to be deduced from other studies.

A possible explanation for the present Gamma distribution is the energy-based criterion of sediment entrainment. Many previous studies considered that sediment entrainment is related to the transfer from the kinetic energy of the near-bed turbulent flow to the potential energy of a bed particle (Hunt, 1999; Valyrakis et al., 2011; Zhong et al., 2012). From this perspective, the Gamma distribution, whose shape factor is $k = 3/2$ (this study) may be better than the Gamma distribution ($k = 2$) used by Armanini et al. (2015) in evaluating the probability of sediment entrainment because a Gamma distribution with $k = 3/2$ is the distribution of the kinetic energy of the ideal gas particles whose velocities follow a Maxwell-Boltzmann distribution. As suggested by Hunt (1999), the near-bed shear stress U_*^2 multiplied by the volume of a particle D^3 can be regarded analogous to the temperature of a thermodynamic system that can be described by Maxwell-Boltzmann statistics. Here, one can treat Ψ_* as a parameter that describes the kinetic energy of the near-bed eddies that have a similar charateristic size as that of the bed particle. The sediment entrainment event is regarded as a heat sink, so the probability distribution of sediment entrainment is characterized by Ψ_* which follows a Gamma distribution with $k = 3/2$. This theoretical model needs to be verified by further experiments that can measure the instantaneous velocities around a particle that is being initiated.

Moreover, the present study not only engenders a modified formula but also proposes a framework to fit an Einstein-type formula to experimental data by calibrating an undetermined probability distribution. As mentioned in Section 3.2, the present data fitting only utilizes partial information of the overall data set. The probability distribution can be determined by the trends of the data with very low and high transport rates. Accordingly, the present framework contains certain merits as follows:

1. The framework shows higher flexibility when fitted to an extended range of experimental data because the type of the probability distribution is flexible, compared with most of the modified formulae that include a presupposed type of probability distribution. If the bed-load transport rates measured in future studies show another trend in the extended range that deviates from the present anticipated trend at the limit (e.g., if the power function (Paintal, 1971) performs better than the exponential function (Einstein, 1942) in predicting $\Phi < 10^{-9}$), the tail of the PDF of Ψ_* can be adjusted correspondingly to fit the updated trend of data.
2. Systematic errors caused by experimental setup and conditions are very common in the laboratory measurements of bed-load transport rate. The present determination of the probability distribution is minimally affected by the systematic errors in the same experimental study, because the probability distribution is determined by only using the gradients obtained from the linear regression of the $\log\Phi - \log\Psi$ (or $\log\Phi - \Psi$) data. If certain biases in Φ are led into by the systematic errors, the corresponding biases in $\log\Phi$ should be identical and do not affect the gradients of the data points.
3. The formula may be improved in future theoretical studies because it is more likely to model the sediment motion when the bed-load transport has extremely low or high mobility than when the transport is moderate. This is because that, in the extreme conditions, the mechanisms are expected to be simple so that more tenable assumptions could be made. If a functional relationship between Φ and Ψ in the extreme conditions is derived, the tails of the PDF of the probability distribution will be determined theoretically. Actually, without theoretical basis, there is inevitable subjectivity in fitting the trends of data at the limits because of the scattering of data points (e.g., whether a power function or an exponential function better fits the data from Paintal (1971)). If some theoretical models can prove the trends of $\Phi(\Psi)$ at the limits, the bed-load formula can be easily improved within the present framework.

Some recent studies on the microscopic sediment motion have investigated the $\Phi(\Psi)$ relation in the extreme conditions. For example, Valyrakis et al. (2011) showed that the sediment entrainment at a location is a Markov process for the very weak bed-load transport and Ancey et al. (2008) shows that the mean travel distance is nearly constant under very weak flow conditions, thus the $\Phi(p)$ relation (Equation 7) assumed by Einstein is accurate if p scales with the particle entrainment rate. Thus, if Valyrakis et al. (2011) could obtain the frequencies of sediment entrainment with more accurate measurements of the mean flow velocities, the $p(\Psi)$ relation can be further determined. Then, the $\Phi(\Psi)$ relation for extremely weak bed-load transport may be derived. On the other hand, Hsu et al. (2004) used the sheet flow to evaluate the intense transport rate and Ali and Dey (2019) studied the scaling law implied in the sediment transport; both studies derived a power law $\Phi(\Psi)$ for intense bed-load transport. It is expected that the further results from these researchers can improve the present formula and add a more robust theoretical basis.

Finally, it is noted that the present framework that fits the tails of PDF to the experimental data is only applicable when there are sufficient data measured in the very low and high transport regimes and based on the assumption that the trends of $\Phi(\Psi)$ at the limits follows the trends of the measured data. It is assumed that the mechanisms of sediment transport do not change significantly for $\Phi < 10^{-9}$ compared with that in $10^{-9} < \Phi < 10^{-3}$ and for $\Phi > 300$ compared with that in $10 < \Phi < 300$.

5. Conclusions

The present study stems from the disagreement between Einstein's bed-load formula and the experimental data with very low and high bed-load transport rate. By rearranging the function in Einstein's model that determines the exchange probability p, the present study shows that a folded Gaussian distribution is embedded in Einstein's formula. Then, a comparison between the calculated limiting forms of Einstein's bed-load formula and the trends of experimental data when the bed-load transport rate approaches 0 and ∞ is conducted. Recognizing that the folded Gaussian distribution causes the disagreement between Einstein's formula and the data, this study explores a probability distribution that renders an Einstein-type formula that better fits the experimental data by replacing the originally assumed probability distribution. Then, the PDF of the folded Gaussian distribution is compared with a PDF deduced from best fitting a smooth curve to the experimental data. The comparison shows the disagreement between the limiting behaviors of the Einstein-assumed probability distribution and the best fit distribution and indicates that the better probability distribution in the modified Einstein-type formula should match the best fit distribution. Based on the

relation between the tails of the PDF and the anticipated trends of experimental data at the limits, it is found that a Gamma distribution can be well fitted to the trends of data with very low and high transport rates. The Gamma distribution is used to replace the original folded Gaussian distribution in Einstein's formula, and a modified Einstein-type formula is determined by fitting its parameters to parts of the data set. Based on the works done in the present study, the following conclusions are drawn:

1. The weakness of the original Einstein's formula in predicting very low and high bed-load transport is inherent in the type of the probability distribution, namely, the folded Gaussian distribution, assumed by Einstein
2. The agreement between an Einstein-type formula and the trends of the $\Phi - \Psi$ data when the bed-load transport rate approaches very low and very high levels are separately related to the limiting behavior of the probability distribution in the formula
3. The modified Einstein-type formula used a Gamma distribution to replace the folded Gaussian distribution (Equation 55), which is calibrated merely by the data with very small and large transport rates (Figure 6), successfully predicts a wide range of bed-load transport rates in $10^9 < \Phi < 300$ (Figure 7)
4. The probability distribution in the present framework is not presupposed but determined only by fitting to trends of the $\Phi - \Psi$ data, which provides a flexible and robust approach to fit an empirical bed-load formula to the experimental data

Data Availability Statement

The bed-load transport rate data in the present article can be obtained from the publications by Gilbert and Murphy (1914), Meyer-Peter and Müller (1948), Wilson (1966), Paintal (1971), Taylor and Vanoni (1972).

Acknowledgments
The first author would gratefully acknowledge the financial support from the NTU Research Scholarship. The authors would also gratefully acknowledge the financial support from the National Natural Science Foundation of China (Grant No. 51979242).

References

Ali, S. Z., & Dey, S. (2019). Bed particle saltation in turbulent wall-shear flow: A review. *Proceedings of the Royal Society A: Mathematical, Physical & Engineering Sciences*, *475*(2223), 20180824. https://doi.org/10.1098/rspa.2018.0824

Ancey, C. (2020). Bedload transport: A walk between randomness and determinism. Part 1: The state of the art. *Journal of Hydraulic Research*, *58*(1), 1–17. https://doi.org/10.1080/00221686.2019.1702594

Ancey, C., Böhm, T., Jodeau, M., & Frey, P. (2006). Statistical description of sediment transport experiments. *Physical Review E*, *74*(1), 011302. https://doi.org/10.1103/PhysRevE.74.011302

Ancey, C., Davison, A. C., Böhm, T., Jodeau, M., & Frey, P. (2008). Entrainment and motion of coarse particles in a shallow water stream down a steep slope. *Journal of Fluid Mechanics*, *595*, 83–114. https://doi.org/10.1017/S0022112007008774

Armanini, A., Cavedon, V., & Righetti, M. (2009). Sediment transport in vegetated rivers. In *33rd IAHR congress: Water engineering for a sustainable environment* (Vol. 1, pp. 888–895).

Armanini, A., Cavedon, V., & Righetti, M. (2015). A probabilistic/deterministic approach for the prediction of the sediment transport rate. *Advances in Water Resources*, *81*, 10–18. https://doi.org/10.1016/j.advwatres.2014.09.008

Bagnold, R. A. (1966). *An approach to the sediment transport problem from general physics*. US Government Printing Office.

Bagnold, R. A. (1983). The nature and correlation of random distributions. *Proceedings of the Royal Society of London. A. Mathematical and Physical Sciences*, *388*, 273–291. https://doi.org/10.1098/rspa.1983.0083

Block, H. W., & Rao, B. R. (1974). Some generalized distributions based on Stacy's generalized gamma distribution. *Scandinavian Actuarial Journal*, *1974*(4), 185–189. https://doi.org/10.1080/03461238.1974.10408680

Bramwell, S. T., Holdsworth, P. C. W., & Pinton, J. F. (1998). Universality of rare fluctuations in turbulence and critical phenomena. *Nature*, *396*(6711), 552–554. https://doi.org/10.1038/25083

Celik, A. O., Diplas, P., Dancey, C. L., & Valyrakis, M. (2010). Impulse and particle dislodgement under turbulent flow conditions. *Physics of Fluids*, *22*(4), 046601. https://doi.org/10.1063/1.3385433

Chen, Y. S., Cheng, N.-S., Liu, X. N., & Wang, S. Q. (1986). Discussion on a modification of Einstein's bed-load function for uniform particles. *Journal of Sediment Research*(3), 87–96.

Cheng, N.-S. (2002). Exponential formula for bedload transport. *Journal of Hydraulic Engineering*, *128*(10), 942–946. https://doi.org/10.1061/(asce)0733-9429(2002)128:10(942)

Chien, N., & Wan, Z. (1999). *Mechanics of sediment transport*. Reston, VA: American Society of Civil Engineers. https://doi.org/10.1061/9780784404003

Crooks, G. E. (2010). *The amoroso distribution*. arXiv preprint arXiv:1005.3274.

Diplas, P., Dancey, C. L., Celik, A. O., Valyrakis, M., Greer, K., & Akar, T. (2008). The role of impulse on the initiation of particle movement under turbulent flow conditions. *Science*, *322*(5902), 717–720. https://doi.org/10.1126/science.1158954

Einstein, H. A. (1942). Formulas for the transportation of bed load. *Transactions of the American Society of Civil Engineers*, *107*(1), 561–577. https://doi.org/10.1061/taceat.0005468

Einstein, H. A. (1950). The bed-load function for sediment transportation in open channel flows (Vol. 1026). Washington, DC:US Department of Agriculture.

Engelund, F., & Fredsøe, J. (1976). A sediment transport model for straight alluvial channels. *Hydrology Research*, *7*(5), 293–306. https://doi.org/10.2166/nh.1976.0019

Forbes, C., Evans, M., Hastings, N., & Peacock, B. (2011). *Statistical distributions*. John Wiley & Sons.

Garimella, R. V. (2017). *A simple introduction to moving least squares and local regression estimation* (Report). Los Alamos, NM: Los Alamos National Lab.

Gilbert, G. K., & Murphy, E. C. (1914). *The transportation of debris by running water*. US Government Printing Office.

Hsu, T.-J., Jenkins, J. T., & Liu, P. L.-F. (2004). On two-phase sediment transport: Sheet flow of massive particles. *Proceedings of the Royal Society of London. Series A: Mathematical, Physical and Engineering Sciences*, *460*(2048), 2223–2250. https://doi.org/10.1098/rspa.2003.1273

Hunt, A. G. (1999). A probabilistic treatment of fluvial entrainment of cohesionless particles. *Journal of Geophysical Research*, *104*(B7), 15409–15413. https://doi.org/10.1029/1999JB900088

Lavelle, J. W., & Mofjeld, H. O. (1987). Do critical stresses for incipient motion and erosion really exist? *Journal of Hydraulic Engineering*, *113*(3), 370–385. https://doi.org/10.1061/(asce)0733-9429(1987)113:3(370)

Meyer-Peter, E., & Müller, R. (1948). Formulas for bed-load transport. In *Proceedings of 2nd meeting of the International Association for Hydraulic Structures Research*, Stockholm.

Nicholas, A. P. (2000). Modelling bedload yield in braided gravel bed rivers. *Geomorphology*, *36*(1), 89–106. https://doi.org/10.1016/s0169-555x(00)00050-7

Paintal, A. S. (1971). Concept of critical shear stress in loose boundary open channels. *Journal of Hydraulic Research*, *9*(1), 91–113. https://doi.org/10.1080/00221687109500339

Schmeeckle, M. W., Nelson, J. M., & Shreve, R. L. (2007). Forces on stationary particles in near-bed turbulent flows. *Journal of Geophysical Research*, *112*, F02003. https://doi.org/10.1029/2006JF000536

Stacy, E. W. (1962). A generalization of the gamma distribution. *The Annals of Mathematical Statistics*, *33*(3), 1187–1192. https://doi.org/10.1214/aoms/1177704481

Taylor, B. D., & Vanoni, V. A. (1972). Temperature effects in low-transport, flat-bed flows. *Journal of the Hydraulics Division*, *98*(8), 1427–1445. https://doi.org/10.1061/jyceaj.0003375

Valyrakis, M., Diplas, P., & Dancey, C. L. (2011). Entrainment of coarse grains in turbulent flows: An extreme value theory approach. *Water Resources Research*, *47*, W09512. https://doi.org/10.1029/2010WR010236

Wang, S. Q. (1985). A modification of Einstein's bed-load function for uniform particles. *Journal of Sediment Research*(1), 44–53.

Wang, X., Zheng, J., Li, D.-x., & Qu, Z. (2008). Modification of the Einstein bed-load formula. *Journal of Hydraulic Engineering*, *134*(9). https://doi.org/10.1061/(asce)0733-9429(2008)134:9(1363)

Wilson, K. C. (1966). Bed-load transport at high shear stress. *Journal of the Hydraulics Division*, *92*(6), 49–59. https://doi.org/10.1061/jyceaj.0001562

Yalin, M. S. (1972). *Mechanics of sediment transport*. Pergamon Press.

Zhong, D.-Y., Wang, G.-Q., & Zhang, L. (2012). A bed-load function based on kinetic theory. *International Journal of Sediment Research*, *27*(4), 460–472. https://doi.org/10.1016/s1001-6279(13)60005-0